

# Diffusion flames in plane-parallel packed beds

Kouichi Kamiuto \*, Sinji Miyamoto

*Department of Mechanical and Energy Systems Engineering, Oita University, Oita 870-1192, Japan*

Received 11 December 2002; received in revised form 2 July 2003

Available online 28 July 2004

## Abstract

Profiles of diffusion flames in plane-parallel packed beds were examined theoretically and experimentally. In the analyses, the flame sheet model taking into account mass dispersion within a packed bed was developed to quantify the effects of several system parameters on the flame shape and flame height in a packed bed. Moreover, experiments for methane–oxygen diffusion combustion in a plane-parallel packed bed of alumina spheres were made to estimate actual flame shapes in the packed bed from photographs of the upper surface of the packed bed and to examine the validity of the flame sheet model.

© 2004 Elsevier Ltd. All rights reserved.

*Keywords:* Diffusion flame; Packed bed; Flame sheet model; Flame shape; Flame height; Mass dispersion

## 1. Introduction

Relating to developments of porous radiant burners and regenerative type combustors with lower  $\text{NO}_x$  emissions, fundamental research on the combustion in porous media has been keenly needed [1], and to meet this requirement, numerous experimental and theoretical studies [2–7] have been performed during the past 20 years.

Almost all of the earlier studies, however, were concerned with the premixed combustion in porous media, and little is known about the diffusion combustion in porous media. In fact, only characteristic features of the shapes of diffusion flames in cylindrical packed beds have been revealed in the literature [8].

The purpose of the present study is to expand knowledge on the diffusion flames in packed beds. To this end, profiles of diffusion flames in plane-parallel packed beds are theoretically and experimentally examined. In the analyses, the flame sheet model [9] taking into account mass dispersion within a packed bed is utilized to evaluate the effects of several system

parameters such as a ratio of the half-width of a combustion chamber to the packed-sphere diameter  $\Gamma$ , the Reynolds number  $Re$ , the porosity  $\phi$  and the mass fraction of oxygen at the inlet of a combustion chamber  $Y_{\text{O}_2}$  on the flame shape and flame height in packed beds. In addition, experiments for methane–oxygen diffusion combustion in a plane-parallel packed bed of alumina spheres are made to estimate actual flame shapes in the packed bed and to discuss the predictability of the proposed flame sheet model.

## 2. Theoretical analyses

The basic assumptions introduced for the theoretical analyses are as follows:

1. A combustion chamber consists of a plane-parallel duct randomly packed with uniform, noncatalytic spheres.
2. The porosity distribution through the combustion chamber is uniform and the mean porosity is 0.39, corresponding to the porosity of a packed bed in random packing.
3. Fuel is injected into the combustion chamber through a plane-parallel duct of width  $2y_f$  located centrally

\* Corresponding author. Tel.: +81-97-554-7797; fax: +81-97-554-7790.

E-mail address: [kamiuto@cc.oita-u.ac.jp](mailto:kamiuto@cc.oita-u.ac.jp) (K. Kamiuto).

### Nomenclature

$D_e$	effective molecular diffusion coefficient	$\gamma_m$	lateral mixing function for mass dispersion
$D_d$	mass dispersion coefficient	$\eta$	dimensionless spanwise coordinate ( $= y/y_0$ )
$D_m$	molecular diffusion coefficient	$\eta_c$	dimensionless spanwise position of the flame surface
$d_p$	mean particle diameter	$\eta_f$	dimensionless half-width of a central zone of the burner ( $= y_f/y_0$ )
$E_f$	Eq. (11)	$\nu$	kinematic viscosity
$i$	quantity representing how much weight of oxygen stoichiometrically combines with fuel	$\xi$	dimensionless streamwise coordinate ( $= x/y_0$ )
$K$	dimensionless total lateral diffusion coefficient	$\xi_c$	dimensionless streamwise position of the flame surface
$Re$	Reynolds number ( $= 2y_0u/\mu$ )	$\xi_c^*$	dimensionless flame height
$Sc$	Schmidt number ( $= \nu/D_m$ )	$\xi_{c\infty}^*$	dimensionless flame height at $ReSc \rightarrow \infty$
$u$	Darcy velocity in the $x$ -direction	$\pi$	a ratio of the circumference of a circle to its diameter
$x$	streamwise coordinate	$\phi$	mean porosity
$Y_f$	mass fraction of fuel	$\phi^*$	critical mean porosity given by $\partial K/\partial \phi = 0$
$Y_o$	mass fraction of oxygen	$\Omega_p$	limiting flame height parameter defined by ( $= \gamma_m \xi_{c\infty}^*/\Gamma$ )
$y$	spanwise coordinate		
$y_f$	half-width of the central zone of a burner		
$y_0$	half-width of a burner		
$\Gamma$	a ratio of the half-width of a combustion chamber to the packed-sphere diameter ( $= y_0/d_p$ )		
		<i>Subscript</i>	
		$i$	quantity at the exit of a burner

inside a large plane-parallel duct of width  $2y_0$  through which an oxygen flow occurs.

- Oxidation of the fuel occurs in a thin sheet of space, when the oxidant and the fuel are in stoichiometric proportion.
- Diffusion alone plays a decisive role in determining the shape of the flame and the molecular diffusion coefficient is independent of temperature and composition.
- Velocities of the fuel and oxidant flows are equal and constant within the combustion chamber.

Under the above-mentioned assumptions, the conservation equations of chemical species are reduced to the following form:

$$u \frac{\partial}{\partial x} (Y_f - Y_o/i) = (D_e + D_d) \frac{\partial^2}{\partial y^2} (Y_f - Y_o/i). \quad (1)$$

Here,  $D_e$  and  $D_d$  represent the effective molecular diffusion coefficient and mass dispersion coefficient [10], respectively and these quantities are given as follows:

$$D_e = \phi D_m, \quad (2)$$

$$D_d = \gamma_m d_p u, \quad (3)$$

$$\gamma_m = 0.1161(1 - \phi)^{1.4609}. \quad (4)$$

The boundary conditions to Eq. (1) are

$$\left. \begin{aligned} x = 0, \quad 0 \leq y \leq y_f : \quad Y_f - Y_o/i &= Y_{fi}, \\ y_f < y \leq y_0 : \quad Y_f - Y_o/i &= -Y_{oi}/i, \\ x \geq 0, \quad y = 0, \quad y = y_0 : \quad \frac{\partial}{\partial y} (Y_f - Y_o/i) &= 0, \end{aligned} \right\} \quad (5)$$

where  $Y_{fi}$  and  $Y_{oi}$ , respectively, denote the mass fractions of the fuel and the oxidant at the inlet of the combustion chamber and  $i$  is a quantity representing how much weight of oxygen stoichiometrically combines with fuel.

To rewrite the governing equation in dimensionless form, the following quantities are introduced:

$$\left[ \begin{aligned} K &= (D_e + D_d)/uy_0 = 2(\phi/ReSc + \gamma_m/2\Gamma), \\ Re &= 2y_0u/\mu, \quad Sc = \nu/D_m, \quad \Gamma = y_0/d_p, \\ \eta &= y/y_0, \quad \eta_f = y_f/y_0, \quad \xi = x/y_0. \end{aligned} \right] \quad (6)$$

Here,  $\nu$  represents the kinematic viscosity of a gas and is assumed to be constant, irrespective of the kind of chemical species. The dimensionless total lateral diffusion coefficient  $K$  takes a minimum at  $\phi^* [= 1 - 211.3(\Gamma/ReSc)^{2.1697}]$ , which is obtained by solving  $\partial K/\partial \phi = 0$ : in the molecular diffusion dominant region ( $\phi > \phi^*$ ),  $K$  increases with  $\phi$ , whereas, in the mass dispersion dominant region ( $\phi < \phi^*$ ),  $K$  increases with a decrease in  $\phi$ .

As a result, we obtain the following dimensionless governing equation and relevant boundary conditions:

$$\frac{\partial}{\partial \xi} (Y_f - Y_o/i) = K \frac{\partial^2}{\partial \eta^2} (Y_f - Y_o/i), \quad (7)$$

$$\left. \begin{aligned} \xi = 0, \quad 0 \leq \eta \leq \eta_f : \quad Y_f - Y_o/i &= Y_{fi}, \\ \eta_f < \eta \leq 1 : \quad Y_f - Y_o/i &= -Y_{oi}/i, \\ x \geq 0, \quad \eta = 0, \quad 1 : \quad \frac{\partial}{\partial \eta} (Y_f - Y_o/i) &= 0. \end{aligned} \right\} \quad (8)$$

Since  $K$  is assumed to be constant, Eq. (7) can be solved analytically to yield

$$\begin{aligned} Y_f - Y_o/i &= (Y_{fi} + Y_{oi}/i)\eta_f - Y_{oi}/i \\ &+ \sum_{n=1}^{\infty} \left\{ \frac{\sin(n\pi\eta_f)}{n\pi/2} (Y_{fi} + Y_{oi}/i) \right. \\ &\times \left. \exp[-K(n\pi)^2\xi] \cos(n\pi\eta) \right\}. \end{aligned} \quad (9)$$

The dimensionless flame location denoted by  $(\xi_c, \eta_c)$  is determined by the following equation, which is obtained by letting  $Y_f - Y_o/i = 0$  in Eq. (9).

$$\sum_{n=1}^{\infty} \left\{ \frac{\sin(n\pi\eta_f)}{n\pi/2} \exp \left[ -2 \left( \frac{\phi}{ReSc} + \frac{\gamma_m}{2\Gamma} \right) (n\pi)^2 \xi_c \right] \times \cos(n\pi\eta_c) \right\} = E_f, \quad (10)$$

$$\begin{aligned} E_f &= [(1 - \eta_f)(Y_{oi}/i) - Y_{fi}\eta_f]/(Y_{fi} + Y_{oi}/i), \\ &(-\eta_f \leq E_f \leq 1 - \eta_f). \end{aligned} \quad (11)$$

Note that setting  $\eta_c = 0$  for  $E_f > 0$  and  $\eta_c = 1$  for  $E_f < 0$  in Eq. (10) gives the flame height  $\xi_c^*$ . Detailed mathematical inspection of Eq. (10) reveals that when a combustion chamber is not filled with solid spheres, i.e.,  $\phi = 1$ ,  $\xi_c^*$  becomes infinite as  $ReSc \rightarrow \infty$  so as to hold Eq. (10) true, whereas, in a packed-bed combustor with  $\phi \neq 1$ , there exists a certain limiting value of  $\xi_c^*$ , which is denoted by  $\xi_{c\infty}^*$  from now, even when  $ReSc \rightarrow \infty$ . Introducing the dimensionless flame height parameter  $\Omega_p$  defined by  $\gamma_m \xi_{c\infty}^*/\gamma$  in Eq. (10) yields

$$E_f = \sum_{n=1}^{\infty} \frac{\sin(n\pi\eta_f)}{n\pi/2} \cos(n\pi\eta_c^*) \exp[-\Omega_p(n\pi)^2]. \quad (12)$$

Here,  $\eta_c^*$  takes 0 or 1, depending on a value of  $E_f$ . Obviously,  $\Omega_p$  is a function of  $\eta_f$  and  $E_f$  alone. Moreover,  $\Omega_p$  becomes infinite at  $E_f = 0$ , but becomes zero at  $E_f = -\eta_f$  and  $1 - \eta_f$ .

Eqs. (10) and (12) were solved numerically utilizing a bisection method with an absolute error less than  $2^{-25}$ .

### 3. Experiments

To examine the predictability of the above-mentioned theoretical model for the flame shape in a plane-parallel packed bed, experiments for methane–oxygen diffusion combustion in a packed bed were made. A schematic diagram of the experimental apparatus is

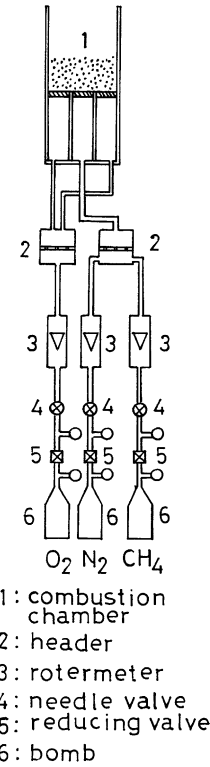


Fig. 1. Schematic diagram of the experimental apparatus.

shown in Fig. 1. The gas burner utilized was of the three flat zone type consisting of a 35 mm wide stainless steel duct with a 10 mm wide stainless steel duct in the middle. The methane–nitrogen mixture entered through the central zone and the oxygen through two outer zones of 10 mm width. Three porous plates were settled at the exit of the burner to support the packed spheres. A box type combustion chamber 35 mm wide, 85 mm long and 150 mm height was attached on the top of the burner. The combustion chamber was made of stainless steel and its outer surface was thermally insulated. Two kinds of alumina sphere (93.0 wt.% and other constituents) with different mean diameters were used as packing material:  $d_p = 2.02$  mm ( $\Gamma = 8.663$ ) and 3.18 mm ( $\Gamma = 5.503$ ). Experimental procedures are as follows: first, to make the combustion chamber empty and then feed methane–nitrogen mixture and oxygen gas at a prescribed velocity. After ignition, pour an amount of alumina spheres randomly to form a packed bed with a constant height. Take photographs of the surface of the combustion chamber from above and then change the height by adding alumina spheres. The mean porosity of the packed bed was found to be about 0.39, as long as the bed height is greater than about 1 cm. The bed height was varied from 0 to 15 cm by a step of 0.5 cm. In addition, gas velocity was varied as follows:  $u = 0.059$  (m/s) ( $Re = 59$ ) and  $u = 0.088$  (m/s) ( $Re = 88.5$ ).

Combustion within the packed bed was always followed by pulsative sounds in a few Hz, and it is presumed from this fact that a flame propagates within the packed bed from the upper surface of the combustor toward the region upstream along the flame sheet and extincts at the exits of the burner and then similar processes are repeated; quasi-steady state diffusion combustion is established within the packed bed. This presumption was confirmed by direct observation of the flame surface formed in a 15 mm thick plane-parallel

packed bed combustor bounded by two transparent silica glass plates, consisting of two 15 mm × 50 mm burners for fuel and oxygen. The fuel and oxygen not exhausted within the packed bed diffusely burned in the free space above the combustor and its flame height decreased with an increase in the bed-height.

Flame shapes within the packed bed were reconstructed from photographs of the upper surface of the packed-bed combustor since, as seen from Fig. 2, two, almost parallel, luminous zones were formed on the upper surface of the combustor and was considered to correspond to locations of the flame surface. However, it was difficult to infer a flame shape near the top of the flame by this method because, as the bed thickness increases, luminous zones become broad and dull, and thus the upper part of a flame shape could not be experimentally determined except for the flame height, which was identified with the bed height where two luminous zones formed on the bed surface just merge.

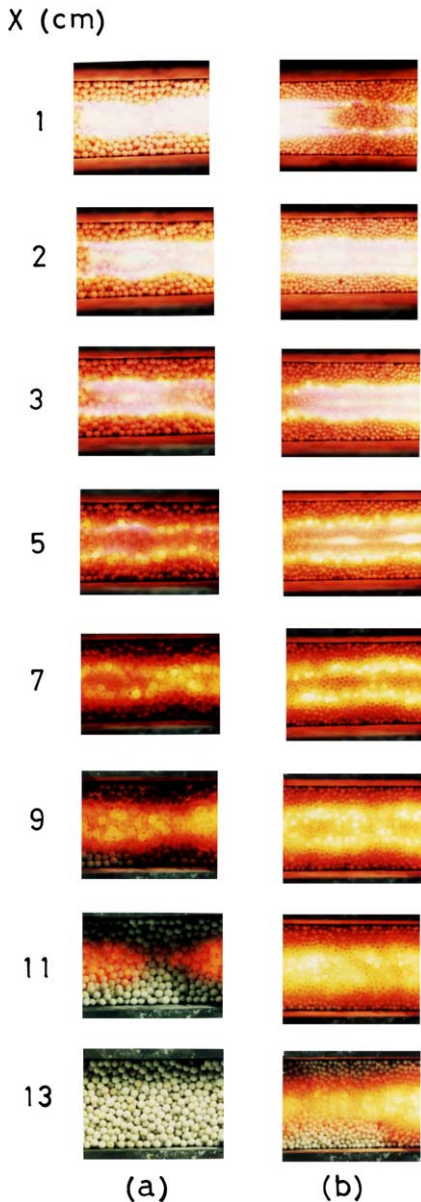


Fig. 2. Photographs of the upper surface of the plane-parallel packed-bed combustor in diffusion combustion: (a)  $\Gamma = 5.503$  and  $Re = 88.5$ , (b)  $\Gamma = 8.663$  and  $Re = 88.5$ .

#### 4. Results and discussion

Comparison between experimentally determined flame shapes and predicted ones is made in Figs. 3 and 4. The arrows in these figures indicate the inferred flame heights. In the theoretical computations, the value of  $i$  was taken to be 3.989, corresponding to the present experimental condition. It is found that the flame shape

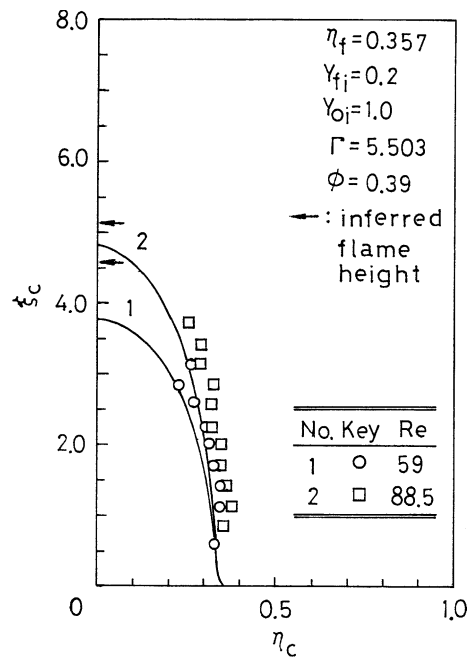


Fig. 3. Comparison between theory and experiment as for profiles of methane–oxygen diffusion flames in the plane-parallel packed-bed combustor with  $\Gamma = 5.503$ .

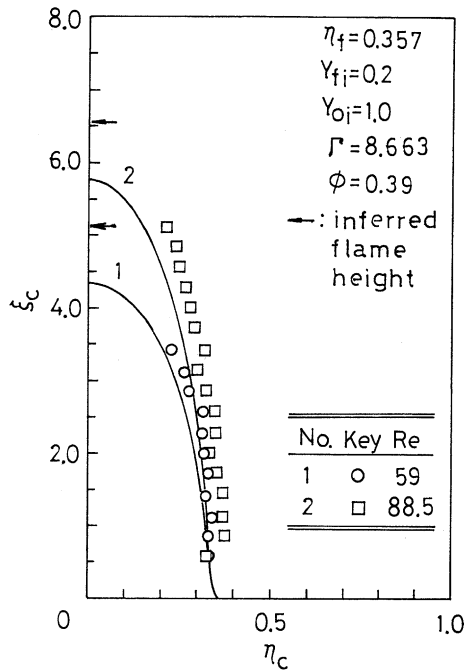


Fig. 4. Comparison between theory and experiment as for profiles of methane–oxygen diffusion flames in the plane-parallel packed-bed combustor with  $\Gamma = 8.663$ .

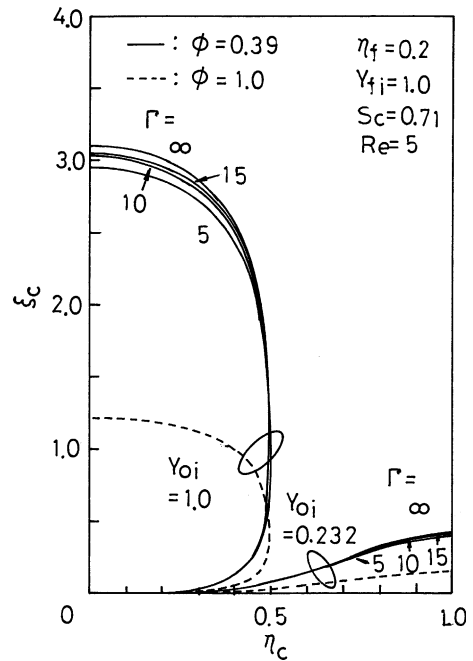


Fig. 5. Predicted profiles of methane–oxygen diffusion flames in packed beds at  $Re = 5$ .

elongates with an increase in  $\Gamma$  and/or  $Re$ . This is caused by the fact that the overall lateral diffusion coefficient of chemical species,  $K$ , becomes small with an increase in  $\Gamma$  and/or  $Re$ . Agreement between theory and experiment is reasonable: the proposed theoretical model adequately predicts the effects of  $\Gamma$  and  $Re$  on the flame shape. The observed discrepancy between theory and experiment is attributable to the effect of thermal radiation which is disregarded in the present study. Here, it should be noted that in order to take into account the effects of thermal radiation on the flame shape theoretically, the conservation equations of mass, momentum and energy must also be solved simultaneously, in addition to the conservation equations of chemical species and therefore simple analytical solutions could not be possibly obtained. Based on the present flame sheet model, the effects of several system parameters such as  $\Gamma$ ,  $Re$ ,  $\phi$  and  $Y_{o,i}$  on the flame shape have been theoretically examined in some detail and the results are illustrated in Figs. 5 and 6. Note that the results for  $Y_{o,i} = 0.232$  show under-ventilated flames, whereas the results for  $Y_{o,i} = 1.0$  represent over-ventilated flames. Typical results for the dimensionless flame height  $\xi_c^*$  are shown in Fig. 7.

The flame height rises with  $\Gamma$  and/or  $ReSc$  and falls with an increase in  $\phi$  as long as  $\phi$  is greater than  $\phi^*$ . However, when  $\phi < \phi^*$ , the flame height increases with  $\phi$  because  $K$  becomes small with an increase in  $\phi$ . Moreover, it is found that, for diffusion flames in packed

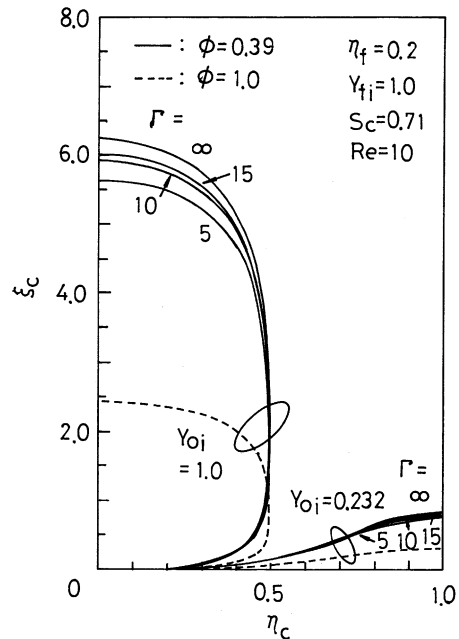


Fig. 6. Predicted profiles of methane–oxygen diffusion flames in packed beds at  $Re = 10$ .

bed with  $\phi \neq 1$ ,  $\xi_c^*$  approaches to a certain limiting value, i.e.,  $\xi_{c,\infty}^*$ , when  $ReSc \rightarrow \infty$ , and this substantiates the aforementioned mathematical conjecture.

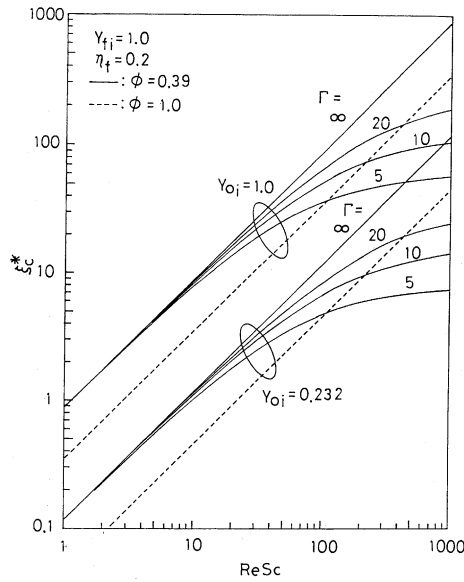


Fig. 7. Relations between  $\xi_c^*$  and  $ReSc$ .

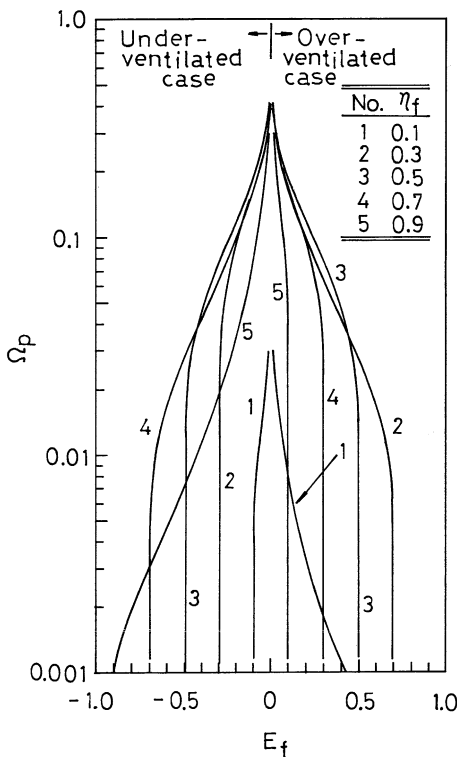


Fig. 8. Relations between  $\Omega_p$  ( $= \gamma_m \xi_{c\infty}^*/\Gamma$ ) and  $E_f$ .

Relations between  $\Omega_p$  ( $= \gamma_m \xi_{c\infty}^*/\Gamma$ ) and  $E_f$  are illustrated in Fig. 8. Since  $E_f = 0$  means that fuel and oxygen are fed into a combustion chamber in stoichiometric

proportion,  $\Omega_p$  increases unlimitedly as  $E_f$  approaches to zero. Corresponding to the overventilated and under-ventilated cases, there exist two values of  $E_f$  for a constant value of  $\Omega_p$ .

### 5. Conclusions

The major conclusions that can be drawn from the present study are as follows:

1. The flame shape in a plane-parallel packed bed elongates with  $\Gamma$  and/or  $Re$  and shrinks with an increase in  $\phi$  as long as  $\phi$  is greater than  $\phi^* [= 1 - 211.3(\Gamma/ReSc)^{2.1697}]$ . However, for  $\phi < \phi^*$ , the flame shape elongates with  $\phi$ .
2. The proposed flame sheet model reasonably predicts the observed effects of  $\Gamma$  and  $Re$  on the flame shape in a plane-parallel packed bed.
3. The proposed flame sheet model predicts that the flame height in a packed bed is finite, even when  $ReSc \rightarrow \infty$ .

### Acknowledgements

The authors wish to express their sincere gratitude to Professor Emeritus R. Echigo, Tokyo Institute of Technology, who encouraged the authors to perform this study. Thanks are also extended to S. Saitoh for his technical assistance in performing the experiment.

### References

- [1] S.S. Penner, A.L. Berland, Fundamental combustion research in support of industrial applications, *Energy—Int. J.* 20 (4) (1995) 311–324.
- [2] R. Echigo, Y. Yoshizawa, K. Hanamura, Analytical and experimental studies on radiative propagation in porous media with internal heat generation, *Heat Transfer* 1986, Hemisphere, Washington, 1986, pp. 827–832.
- [3] Y.-K. Chen, R.D. Mattheus, J.R. Howell, The effect of radiation on the structure of premixed flame within a highly porous inert media, *ASME, HTD* 81 (1987) 35–42.
- [4] T.W. Tong, S.B. Sathé, Heat transfer characteristics of porous radiant burners, *ASME J. Heat Transfer* 113 (2) (1991) 423–428.
- [5] K. Hanamura, R. Echigo, S.A. Zhdanok, Super adiabatic combustion in porous media, *Int. J. Heat Mass Transfer* 36 (12) (1993) 3201–3209.
- [6] J.R. Howell, M.J. Hall, J.L. Ellzery, Combustion of hydrocarbon fuels within porous inert media, *Prog. Energy Combust. Sci.* 22 (1996) 121–145.
- [7] R. Viskanta, J.P. Gore, Overview of cellular ceramics based porous radiant burners for supporting combustion, *Environ. Combust. Technol.* 1 (2000) 167–203.

- [8] K. Kamiuto, T. Ogawa, Diffusion flames in cylindrical packed beds, *AIAA J. Thermophys. Heat Transfer* 11 (4) (1997) 585–587.
- [9] S.P. Burke, T.E.W. Schumann, Diffusion flames, *Ind. Eng. Chem.* 20 (10) (1928) 998–1005.
- [10] K. Kamiuto, S. Saitoh, Simultaneous heat and mass transfer in packed bed catalytic reactor, *AIAA J. Thermophys. Heat Transfer* 9 (3) (1995) 524–530.